PHYSICAL REVIEW D VOLUME 19, NUMBER 5 1 MARCH 1979

Transverse-momentum correlations and impact-parameter bounds for exclusive K^+p reactions at 32 GeV/c

E. A. De Wolf,* M. Gysen, S. Tavernier, and F. Verbeure*
Interuniversity Institute for High Energies, ULB-VUB, Brussels, Belgium

I. V. Ajinenko, P. V. Chliapnikov, L. N. Gerdyukov, S. B. Lugovsky, V. N. Riadovikov, A. M. Rybin, O. G. Tchikilev, and A. B. Vorobjev
Institute for High Energy Physics, Serpukhov, U.S.S.R.

C. Dujardin, F. Grard, and J. Laurent
Université de l'État, Mons, Belgium

M. De Beer and J. Ph. Laugier
Centre d'Études Nucléaires, Saclay, France
(Received 25 September 1978)

The Webber and Henyey-Pumplin lower bounds on the root-mean-square impact parameter of exclusive K^+p reactions are determined and compared with the slope of the overlap function calculated from uncorrelated-particle-production models. The similarity of the lower bounds obtained with different methods is shown to be a consequence of the nearly Gaussian transverse-momentum structure of the reaction matrix element squared at fixed rapidities. Multiplicity and total-energy dependence follow naturally from the dynamical transverse-momentum limitation and phase space. The weakness of the lower bounds constitutes evidence for important phase and/or spin contributions to the average squared impact parameter.

I. INTRODUCTION

The study of the impact-parameter structure of elastic and inelastic hadron collisions at high energy has attracted much attention in recent years. Impact-parameter analyses of elastic scattering data in the Fermilab and CERN ISR energy range, combined with s-channel unitarity, revealed interesting properties of elastic, inelastic, and diffractive processes.[1-3] Unfortunately, very little is known about the angular-momentum (or impact-paramater) dependence of exclusive inelastic reaction channels. In particular, it has not been possible to decide whether high-multiplicity reactions are indeed more central than low-multiplicity reactions as one expects on intuitive grounds. Similarly, the interesting possibility that $\bar{p}p$ annihilation could mainly be a peripheral process, as seems to follow from a comparison of $\bar{p}p$ and pp elastic scattering,[4] is not yet established. The reason for our lack of information is well known[5-7] and follows from the fact that the total-angular-momentum dependence of many particle reactions is not only determined by the modulus of the reaction matrix element but also by the momentum-dependent phase, which is usually unobservable. If the multiparticle phases vary sufficiently fast as a function of the momenta of final-state particles, one is confronted with a situation where almost all angular momentum or impact-parameter characteristics remain hidden in unmeasurable properties of the reaction matrix element.[8-12]

Nevertheless, several methods were recently proposed[13-17] to determine lower bounds on $\langle J^2\rangle$, the average of the total angular momentum squared in a certain reaction. The corresponding average impact parameter squared $\langle b^2\rangle$ is then defined as

$$\langle b^2\rangle = \langle J^2\rangle / p^2 \,, \tag{1}$$

where p is c.m.s. momentum of the incoming particles.[18]

A simple lower bound, adequate for exclusive reactions, was first proposed by Webber[13] and has already been studied at various energies in a variety of reactions with different beams and number of particles in the final state.[19-24] From such studies it was found that the Webber bounds generally decrease when the multiplicity increases, and increases with growing incident momentum, at fixed multiplicity. Smaller values of the bound were obtained for annihilation processes. Unfortunately, the smallness of the lower bounds, in comparison with the $\langle b^2\rangle$ deduced from elastic scattering, makes any conclusions about the behavior of the real rms impact parameter quite unreliable.

Recently, Webber's method was criticized by Henyey and Pumplin.[14] They remarked that his bound is inadequate when absorptive mechanisms

are present and therefore proposed an alternative lower bound which, according to the authors, would be close to the real r.m.s. impact parameter.

In the present paper we study the reactions

(a) $K^+p \to K^+p\pi^+\pi^-$,

(b) $K^+p \to K^+p\pi^+\pi^+\pi^-\pi^-$,

(c) $K^+p \to K^+p\pi^+\pi^+\pi^+\pi^-\pi^-\pi^-$.

at incident K^+ momenta of 8.2, 16, and 32 GeV/c. We will show that the expectations of Henyey and Pumplin are not confirmed by our experimental data. In order to understand more clearly the significance of the results we further determine the lower bounds on the rms impact parameter with a technique similar to the one used by Michejda,[5] and based on the calculation of the Van Hove overlap function.[6]

The paper is organized as follows. In Sec. II we describe the experimental data sample used in this analysis, discuss single-particle characteristics and transverse-momentum correlations, and compare the data with predictions of uncorrelated-particle-production models. In Sec. III we present our results on the Webber and Henyey-Pumplin bounds and compare them with the bounds calculated from the overlap function. The discussion of the results and our conclusions are given in Sec. IV.

II. DATA SAMPLE AND GENERAL CHARACTERISTICS

A. Data sample

The experimental data at 32 GeV/c are the result of a 400 000 pictures exposure of the hydrogen bubble chamber Mirabelle to a rf separated K^+ beam at 32.1 GeV/c at the Serpukhov accelerator. This film was double-scanned and measured on semiautomatic film-plane digitizers or on Hough-Powell devices. With the present statistics of about 5 events/μb we obtained 2677, 651, and 179 events of the four-constraint (4C) reactions (a), (b), and (c), respectively. The K^+/π^+ identification ambiguity, which happens in about 25% of reaction (a) at 32 GeV/c, as well as ambiguities between three competing 4C-fit hypotheses (6%) have been resolved by accepting all hypotheses compatible with the observed bubble density and using a weight $\frac{1}{2}, \frac{1}{3}$ for the K/π identification. No attempt was made to correct for some losses of events (9% at 32 GeV/c) with unseen recoil proton for reaction (a).

The data on reactions (a) and (b) at 8.2 and 16 GeV/c have been obtained in exposures of the CERN 2-m H_2 bubble chamber to rf-separated K^+ beams at the CERN Proton Synchrotron. In this analysis a sample of 7550 and 14 060 events of reaction (a) and 1211 and 1178 events of reaction (b) at 8.2 and 16 GeV/c, respectively, were used. Details on these experiments may be found elsewhere.[25]

B. Single-particle distributions

The single-particle distributions for reactions (a) and (b) exhibit the well known properties of all multiparticle hadron collisions in our energy range.

(i) Distributions of the transverse momentum $\vec{k}_i$ of particle i ($i=p, K^+, \pi^+, \pi^-$) show an approximately exponential behavior in k_i^2 (Fig. 1). The width of these distributions depends rather strongly on the c.m.s. rapidity y_i or the c.m.s. longitudinal momentum fraction (Feynman variable) x_i and on the mass of the particle. This is illustrated by Fig. 2 where, as an example, $\langle k_i^2(y_i)\rangle$ for reaction (a) at 32 GeV/c is presented. These data are compared with an uncorrelated jet model with matrix element squared

$$|M|^2 = \prod_{i=1}^{n} \exp(-\beta_i k_i^2), \tag{2}$$

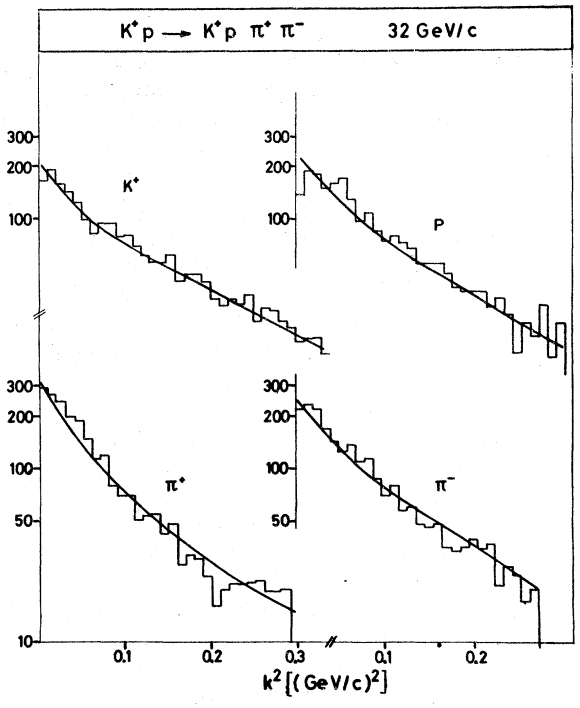

FIG. 1. Distributions of the transverse momentum squared in reaction (a) at 32 GeV/c. The curves are the predictions of model (4), see text.

TABLE I. (a) Single-particle characteristics of reaction $K^+p \to K^+p\,\pi^+\pi^-$ at 8.2, 16, and 32 GeV/c; (b) and (c) the same for reactions $K^+p \to K^+p\,2(\pi^+\pi^-)$ and $K^+p \to K^+p\,3(\pi^+\pi^-)$, respectively.

(a) $K^+p \to K^+p\pi^+\pi^-$

	Experimental values $\langle k^2 \rangle$ [(GeV/c)^2]	$\langle x \rangle$	Model (2) β_i [(GeV/c^{-2})]
	8.2 GeV/c		
p	0.184 ± 0.003	−0.652 ± 0.003	3.6
K^+	0.199 ± 0.003	0.462 ± 0.004	3.0
π^+	0.127 ± 0.002	0.032 ± 0.003	5.6
π^-	0.133 ± 0.002	0.158 ± 0.003	5.3
λ	3.735 ± 0.009		4.187 ± 0.006
	16 GeV/c		
p	0.153 ± 0.002	−0.777 ± 0.002	4.8
K^+	0.189 ± 0.002	0.531 ± 0.003	3.1
π^+	0.131 ± 0.002	0.101 ± 0.002	5.4
π^-	0.136 ± 0.002	0.145 ± 0.002	5.15
λ	5.317 ± 0.007		5.36 ± 0.01
	32 GeV/c		
p	0.167 ± 0.004	−0.791 ± 0.005	4.3
K^+	0.203 ± 0.005	0.597 ± 0.006	3.0
π^+	0.130 ± 0.004	0.077 ± 0.006	5.7
π^-	0.145 ± 0.004	0.117 ± 0.006	5.0
λ	5.389 ± 0.025		5.724 ± 0.016

(b) $K^+p \to K^+p\,2(\pi^+\pi^-)$

	Experimental values $\langle k^2 \rangle$ [(GeV/c)^2]	$\langle x \rangle$	Model (2) β_i [(GeV/c)^2]
	8.2 GeV/c		
p	0.250 ± 0.009	−0.269 ± 0.008	2.0
K^+	0.216 ± 0.008	0.197 ± 0.008	2.0
π^+	0.136 ± 0.004	−0.005 ± 0.005	3.6
π^-	0.126 ± 0.003	0.041 ± 0.005	4.0
λ	1.080 ± 0.013		1.378 ± 0.002
	16 GeV/c		
p	0.234 ± 0.007	−0.492 ± 0.008	3.0
K^+	0.262 ± 0.006	0.314 ± 0.008	2.3
π^+	0.169 ± 0.004	0.021 ± 0.005	3.8
π^-	0.157 ± 0.004	0.068 ± 0.004	4.3
λ	2.186 ± 0.017		2.331 ± 0.002
	32 GeV/c		
p	0.206 ± 0.009	−0.585 ± 0.012	3.7
K^+	0.234 ± 0.010	0.395 ± 0.013	2.9
π^+	0.173 ± 0.007	0.021 ± 0.007	4.0
π^-	0.161 ± 0.006	0.074 ± 0.006	4.5
λ	3.35 ± 0.24		3.330 ± 0.002

TABLE I. (*Continued*)

	(c) $K^+p \to K^+p\,3(\pi^+\pi^-)$		
	$\langle k^2 \rangle$ [(GeV/c)^2]	Experimental values $\langle x_i \rangle$	Model (2) β_i [(GeV/c)$^{-2}$]
		32 GeV/c	
p	0.247 ± 0.015	−0.377 ± 0.024	3.0
K^+	0.222 ± 0.016	0.163 ± 0.022	3.5
π^+	0.156 ± 0.009	0.024 ± 0.008	4.5
π^-	0.158 ± 0.010	0.047 ± 0.007	4.5
λ		2.10 ± 0.12	2.448 ± 0.007

with n = number of final-state particles. The constant parameters β_i were chosen in order to reproduce the experimental *global* averages $\langle k_i^2 \rangle$. The values of β_i together with the experimental $\langle k_i^2 \rangle$ for reactions (a)–(c) are collected in Table I. They show considerable dependence on particle type, multiplicity and incident energy. As seen from Fig. 2, the simple model (2) accounts for most of the rapidity dependence of $\langle k_i^2(y_i) \rangle$ in reaction (a) at 32 GeV/c, although deviations are observed. The agreement is also good at 8.2 and 16 GeV/c, especially for the higher multiplicity reactions.

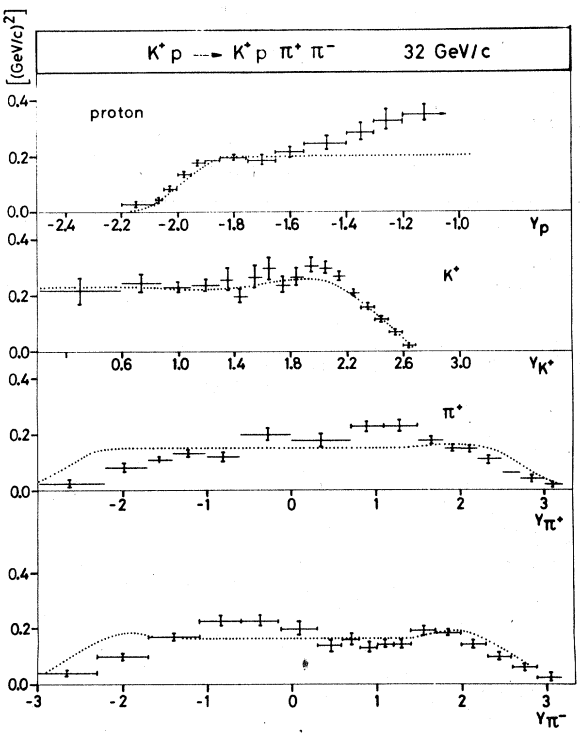

FIG. 2. Rapidity dependence of the average transverse momentum squared for all final-state particles in the reaction $K^+p \to K^+p\pi^+\pi^-$. The curves are predictions of model (2), see text.

(ii) The rapidity and Feynman-x distributions (not shown) exhibit the usual strong leading-particle effects for protons and kaons (the latter being less leading), while pions are centrally produced. These properties are illustrated by the values of the averages $\langle x_i \rangle$ collected in Table I. Evidently, model (2) completely fails to account for the longitudinal distributions in our data since no leading particle effects were introduced. Nevertheless, it is interesting to note that the experimental value of

$$\lambda = \left\langle \sum_{i=1}^{n} \beta_i x_i^2 \right\rangle$$

is quite close to the model prediction (see Table I). This proves that leading particles have only weak influence on the value of λ which, as will become clear in Sec. III, essentially determines the lower bound on the rms impact parameter.[26]

C. Transverse-momentum correlations

1. Experimental results

Since dynamical transverse-momentum correlations are expected to play an important role in impact-parameter determinations[27] and are of some interest in their own right, we briefly discuss some relevant results for the reactions (a) and (b).[28]

Figure 3 shows the distributions of the correlation matrix elements T_{ij} $(i \neq j)$ defined as

$$T_{ij} = \vec{k}_i \cdot \vec{k}_j \qquad (3)$$

$(i, j = p, K^+, \pi^\pm)$ for reaction (a) at 32 GeV/c. These distributions are approximately exponential in T_{ij} separately for $T_{ij} < 0$ and $T_{ij} > 0$, but with a larger slope in the latter case (see also the Appendix). The averages $\langle T_{ij} \rangle$ $(i \neq j)$ are presented

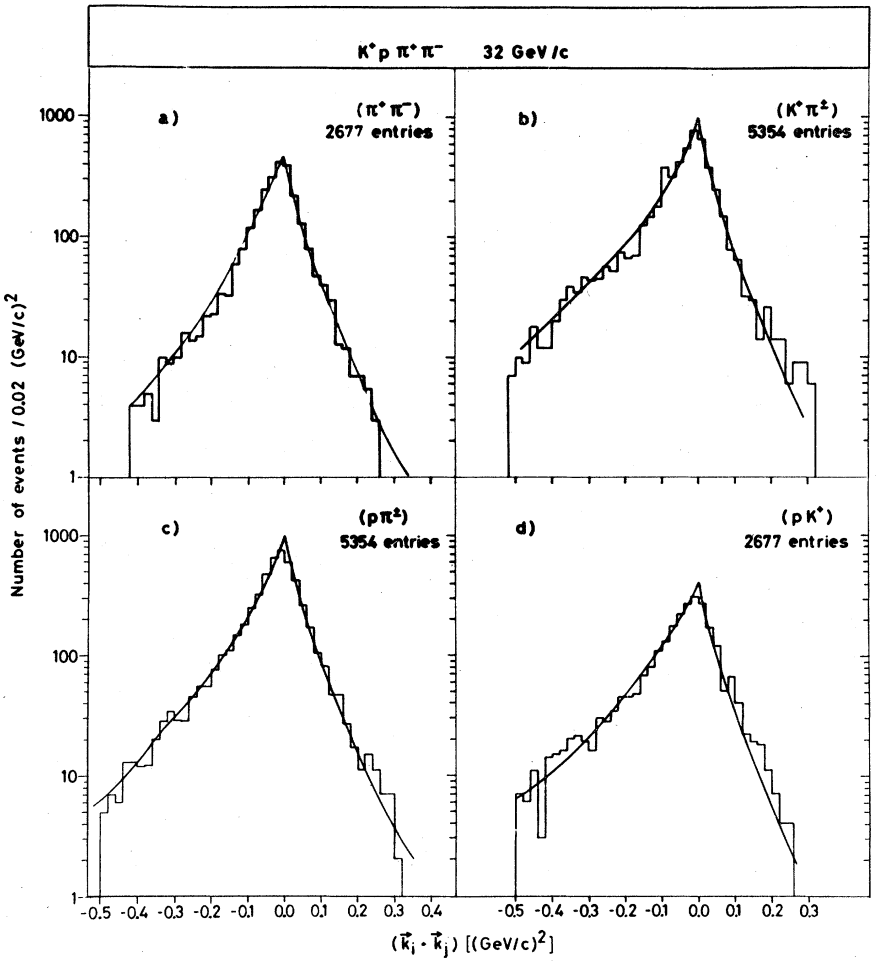

FIG. 3. Distribution of scalar products of transverse momenta for various combinations of particles in the reaction (a) at 32 GeV/c. The curves are predictions of model (4), see text.

in Figs. 4(a), and 4(b) as a function of rapidity difference $\Delta y = |y_i - y_j|$ for all two-particle combinations in reactions (a) and (b), respectively, at 32 GeV/c. The data exhibit important transverse-momentum correlations, expecially between the leading particles, when the rapidity separation is small. Similar effects are present in reactions (a) and (b) at 8.2 and 16 GeV/c.

2. *Comparison with uncorrelated models*

To investigate whether the observed correlations are of dynamical or kinematical origin, we have studied the consequences of the hypothesis that all transverse momenta are uncorrelated. To this end we first considered model (2) and found no satisfactory agreement neither for the T_{ij} distributions nor for the Δy dependence of $\langle T_{ij} \rangle$, which is predicted to be essentially constant. Since the failure of this model was found to be due to the neglect of dynamical rapidity correlations and rapidity dependence of the parameters β_i, we adopted the approach of Ref. 30 and considered a model for which the differential probability distribution is written as

$$\frac{1}{\sigma_n}\frac{d\sigma_n}{d^2k_1 \cdots d^2k_n dy_1 \cdots dy_n} = 2\pi A^2(y_1, \ldots, y_n) F(y_1, \ldots y_n) \prod_{i=1}^{n} W(\vec{k}_i, y_i) \delta^2\left(\sum_{i=1}^{n} \vec{k}_i\right) . \quad (4)$$

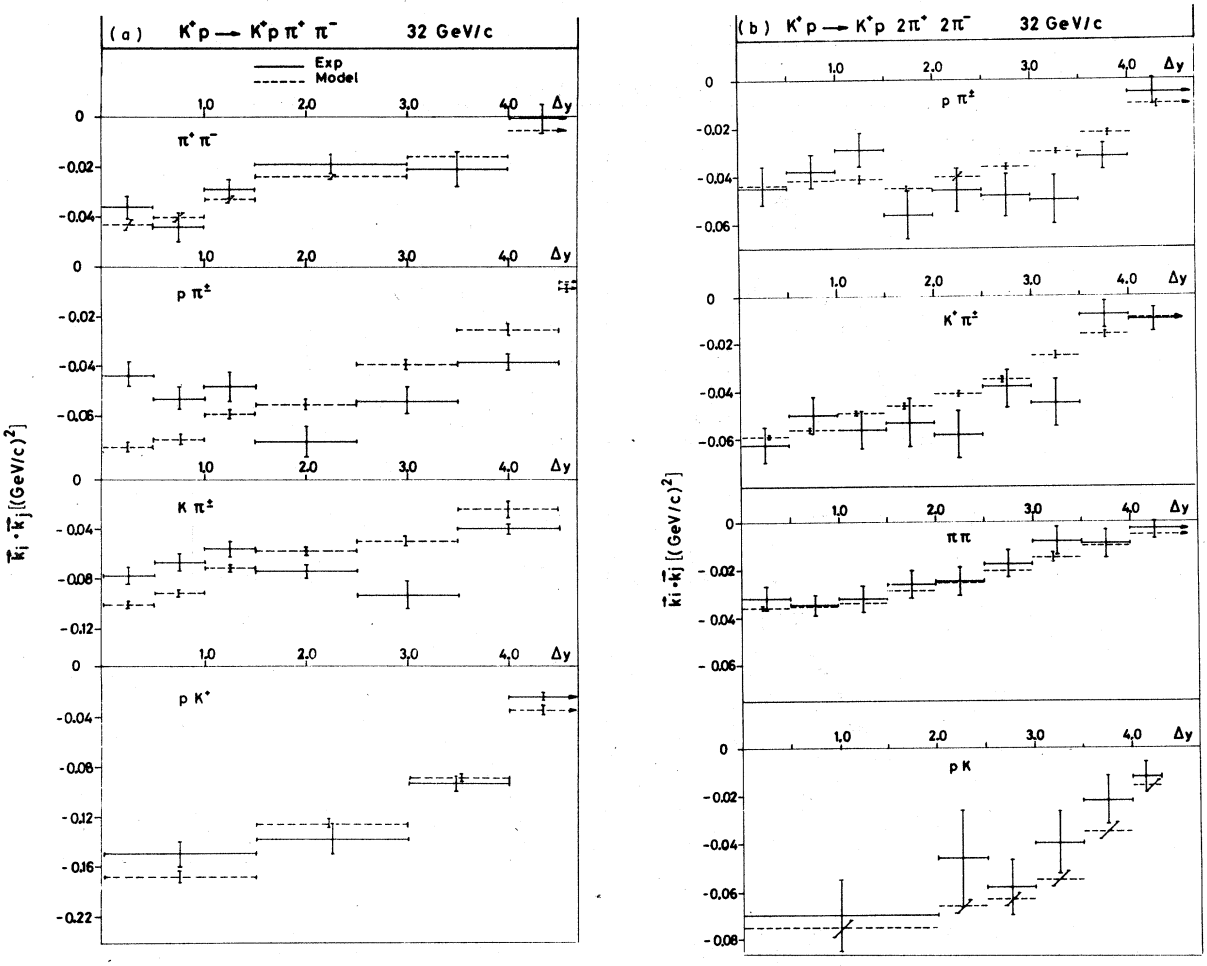

FIG. 4. (a) Dependence of the $\langle T_{ij} \rangle$ on Δy in reaction (a) at 32 GeV/c. The dashed lines are predictions of model (4), see text. (b) same as in (a) for reaction (b) at 32 GeV/c.

$W(\vec{k}, y)$ describes the transverse-momentum distribution at rapidity y. We assumed the Gaussian form

$$W(\vec{k}, y) = \frac{1}{2\pi a^2(y)} \exp[-k^2/2a^2(y)] \,. \tag{5}$$

$F(y_1, \ldots, y_n)$ is the marginal rapidity distribution normalized to 1. This function contains all possible correlations between rapidities of initial- and final-state particles. The factor $2\pi A^2(y_1, \ldots, y_n)$ with

$$A^2(y_1, \ldots, y_n) = \sum_{i=1}^{n} a_i^2(y_i) \tag{6}$$

takes care of normalization. From (4) and (5) one obtains analytical expressions at fixed y_i for all quantities or distributions of interest. The functions $a_i^2(y_i)$, the only unknowns in the model, can be determined, e.g., by iterations, from the corresponding experimental values of $\langle k_i^2(y_i) \rangle$. For more details we refer to the Appendix.

The results obtained from model (4) at 32 GeV/c are shown in Figs. 1 and 3 (solid lines) and in Fig. 4 (dashed lines). Excellent agreement is found for all rapidity integrated distributions. The model also accounts quite well for the absolute values and rapidity dependence of the averages $\langle T_{ij} \rangle$ $(i \neq j)$. This is particularly true for the correlations between the leading K^+ and proton. Nevertheless, some evidence for (not unexpected) dynamical correlations between $(K\pi)$ and $(p\pi)$ pairs is seen, but these are rather small. Similar overall agreement was found at 8.2 and 16 GeV/c.

The results of this section clearly show that a particle production model which incorporates

all experimental rapidity correlations and assumes absence of dynamical transverse momentum correlations at fixed rapidities, describes very well the transverse-momentum structure of the exclusive reactions.[31] This provides other evidence against[29,30,32] the hypothesis of local compensation of transverse momentum,[15-17] at least in our energy range. Our analysis also indicates that no meaningful tests of short-range order in transverse momentum are possible unless rapidity correlations and rapidity dependence of the transverse-momentum distributions are taken into account. Some of these features were neglected in a recent analysis of local conservation of transverse momentum at Fermilab energies.[32b]

III. DETERMINATION OF LOWER BOUNDS ON THE RMS IMPACT PARAMETER

A. Definitions, maximum and minimum bounds

As was first shown by Van Hove,[6] it is possible to determine the "partial-wave" cross sections σ_J^n of a n-body reaction initiated by incoming particles with total angular momentum J, from the corresponding overlap function $F_n(t)$ defined as[33]

$$F_n(t) = \int M_n^*(\vec{p}_1, \ldots, \vec{p}_n) M_n(R\vec{p}_1, \ldots, R\vec{p}_n) d\chi_n , \tag{7}$$

where $M_n(p_1, \ldots, p_n)$ is the reaction matrix element. The operator R rotates the c.m.s. momenta of final-state particles over an angle θ around an axis perpendicular to the incident particle direction; t represents the corresponding elastic energy-momentum transfer $[t = -4p^2 \sin^2(\frac{1}{2}\theta)]$; $d\chi_n$ is the phase-space volume element.

The average impact parameter squared, defined as

$$\langle b_n^2 \rangle = \frac{1}{p^2} \sum_J J(J+1)\sigma_J^n / \sum_J \sigma_J^n , \tag{8}$$

is directly proportional to the slope of the overlap function and given by

$$\langle b_n^2 \rangle = 4[d \ln F_n(t)/dt]_{t=0} . \tag{9}$$

The phase of the matrix element M_n contributes a positive-definite term to $\langle b_n^2 \rangle$.[7] Consequently, only a lower bound on $\langle b_n^2 \rangle$ will be obtained if M_n in (7) is replaced by its (measurable) modulus. This lower bound will be called "maximum bound."[14] On the other hand, it has been noted[32a] that for given transverse-momentum distributions, a "minimum bound" exists which can be

TABLE II. Lower bound on r.m.s. impact parameter (in fm) obtained with different methods for reactions (a), (b), and (c) at 8.2, 16, and 32 GeV/c.

(1) Bounds Reaction	(2) $\langle \sum \beta_i x_i^2 \rangle_{\text{expt}}^{1/2}$	(3) "Minimum" bound	(4) Webber bound	(5) HP bound	(6) HP bound model (2)	(7) HP, $\tau_{\min}$ Model (2)	(8) Overlap method
$K^+p \to K^+p\pi^+\pi^-$, 8.2 GeV/c	0.381±0.001	0.36 ±0.02	0.32±0.01	0.41±0.03	0.330±0.015	0.52±0.05	0.406±0.004
$K^+p \to K^+p\,2(\pi^+\pi^-)$, 8.2 GeV/$c$	0.205±0.001	0.17 ±0.02	0.16±0.01	0.19±0.07	0.20 ±0.02	0.40±0.05	0.27 ±0.03
$K^+p \to K^+p\pi^+\pi^-$, 16 GeV/c	0.455±0.001	0.44 ±0.01	0.41±0.01	0.45±0.05	0.373±0.016	0.52±0.05	0.453±0.004
$K^+p \to K^+p\,2(\pi^+\pi^-)$, 16 GeV/$c$	0.292±0.001	0.271±0.005	0.24±0.02	0.25±0.06	0.24 ±0.02	0.42±0.04	0.30 ±0.05
$K^+p \to K^+p\pi^+\pi^-$, 32 GeV/c	0.458±0.001	0.47 ±0.01	0.40±0.01	0.45±0.04	0.40 ±0.02	0.60±0.05	0.471±0.006
$K^+p \to K^+p\,2(\pi^+\pi^-)$, 32 GeV/$c$	0.361±0.001	0.34 ±0.02	0.31±0.02	0.36±0.06	0.29 ±0.02	0.52±0.03	0.37 ±0.05
$K^+p \to K^+p\,3(\pi^+\pi^-)$, 32 GeV/$c$	0.286±0.08	0.28 ±0.01	0.25±0.03	0.42±0.15	0.24 ±0.02	0.46±0.06	

derived from the Gaussian matrix element

$$G_n(\vec{p}_1, \ldots, \vec{p}_n) = A \exp\left(-\tfrac{1}{2} \sum_{i,j} C_{ij} \vec{k}_i \cdot \vec{k}_j\right), \quad (10)$$

where A and C_{ij} are real functions of longitudinal momenta or rapidities. The coefficient C_{ij} should be such that model (10) reproduces the given $\langle k_i^2 \rangle$ values at each point in longitudinal phase space. The "minimum bound" at fixed longitudinal momenta is approximately equal to[34]

$$b_M^2 = \sum_{i,j=1}^{n} C_{ij} x_i x_j \,, \quad (11a)$$

which may well be approximated by

$$b_M^2 = \sum_{i=1}^{n} \beta_i x_i^2, \quad \beta \equiv C_{ii} \quad (11b)$$

since dynamical transverse-momentum correlations are found to be small. The average "minimum bound," $\langle b_M^2 \rangle$, integrated over total longitudinal phase space can easily be obtained from direct (e.g., Monte Carlo) calculation of the overlap function (7) with matrix element (10).

Average "minimum bounds" for reactions (a)–(c) at 8.2, 16, and 32 GeV/c were calculated with this method using model (2) and the β_i values from Table I. They are collected in Table II, column 3 together with the corresponding experimental $\langle b_M^2 \rangle_{\text{expt}}^{1/2}$ (column 2) derived from (11b). Both quantities almost coincide for a given reaction and energy and moreover show pronounced energy and multiplicity dependence. Comparison of these "minimum bounds" with other lower bounds will allow us to appreciate the relative merits of different "optimized" methods presented in the literature.[35]

B. Webber and Henyey-Pumplin bounds

The "maximum bound" discussed in the previous section is defined in terms of the overlap function and cannot be obtained from experiment unless the modulus of the amplitude is known. Since this is unfeasible with the presently available statistics, other methods have been proposed to determine experimental lower bounds in a model-independent way.

In the first one, proposed by Webber,[13] and already applied to a variety of exclusive reactions,[19-24] the lower bound $\langle b_W^2 \rangle^{1/2}$ on the rms impact parameter is written as[14]

$$\langle b_W^2 \rangle = \sum_{i=1}^{n-1} u_i \langle x_i \rangle \,. \quad (12)$$

The arbitrary functions u_i serve to optimize the bound and have been determined from the set of equations:

$$\langle x_i \rangle = \sum_{j=1}^{n-1} \langle T_{ij} \rangle u_j \,. \quad (13)$$

The matrix T is defined in Sec. II C. The averages in (12) and (13) should in principle be calculated in as many small regions of longitudinal phase space as allowed by statistics. The Webber bound (12) coincides with the "minimum bound" (Sec. III A) provided $(T^{-1})_{ij} = C_{ij}$. Experimentally, this equality will only be satisfied as long as energy-momentum conservation effects remain negligible. Consequently, determination of Webber's bound in fragmentation regions or at the edge of phase space generally leads to an overestimation of the lower bound which cannot easily be corrected.

A superior bound was derived by Henyey and Pumplin (HP).[14] In their approach one starts from a set of $(n-1)$ arbitrary functions u_i of the longitudinal momenta and defines the variable

$$\tau = \sum_{i=1}^{n-1} (u_i \vec{k}_i)^2 \Big/ \left(\sum_{i=1}^{n-1} u_i x_i\right)^2 \quad (14)$$

calculated for each event. The HP bound is then given by

$$\langle b_{\text{HP}}^2 \rangle = \left\langle \tau \left(\frac{d}{d\tau} \ln \frac{d\sigma}{d\tau}\right)^2 \right\rangle, \quad (15)$$

where $d\sigma/d\tau$ is the experimental τ distribution. The average in (15) may either be calculated numerically, once $d\sigma/d\tau$ has been parametrized, or may be evaluated, as in our case, by taking the average over all experimental events. For the parametrization of $d\sigma/d\tau$ we adopted the expression

$$d\sigma/d\tau = \exp\left(\sum_k A_k \tau^k\right) \quad (k \geq 0) \,, \quad (16)$$

which provided adequate fits to all our data.

The HP bound coincides with the Webber bound and with the "minimum bound" for a Gaussian matrix element of the form (10).

C. Experimental results

1. *Webber bounds*

The Webber bounds for reactions (a)–(c) at 8.2, 16, and 32 GeV/c were calculated from (12) and (13) by averaging over *all events*. They are collected in Table II and compared with corres-

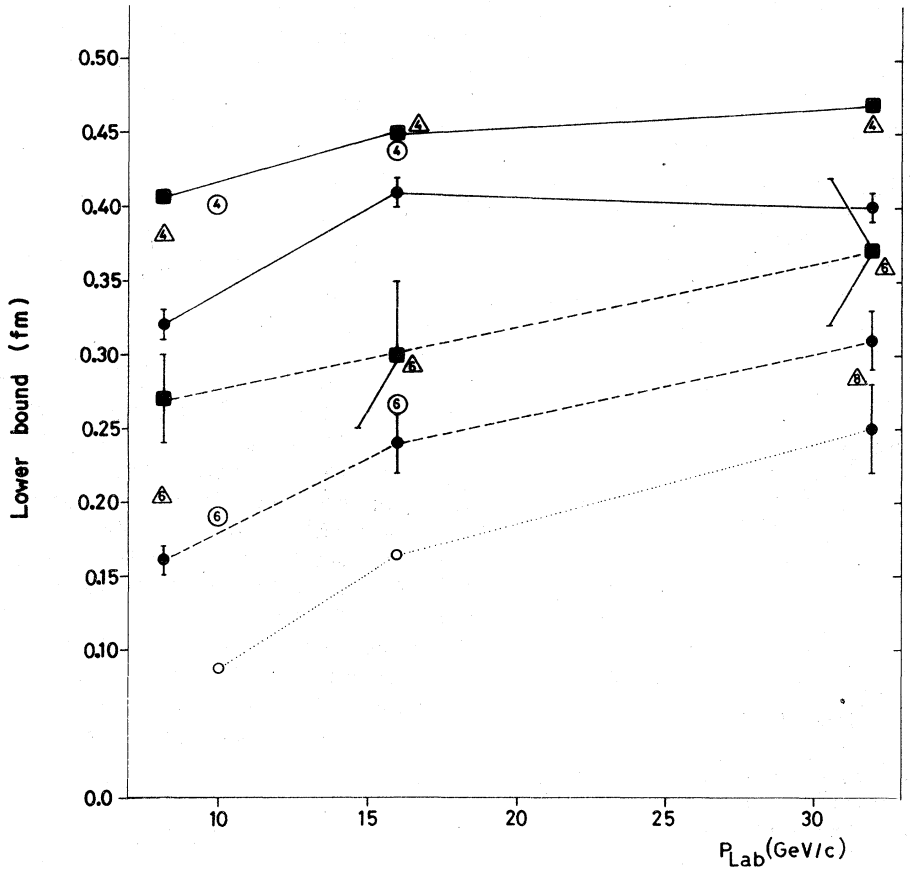

FIG. 5. Lower bounds on rms impact parameter for reactions (a)-(c) and comparison with corresponding K^-p reactions. ● (○) Webber bounds for K^+p (K^-p) reactions; figures in symbols indicate multiplicity of reaction. ■ Overlap-function bounds for K^+p reactions. Δ "lower bounds" equal to experimental value of $\langle \sum \beta_i x_i^2 \rangle^{1/2}$. Full lines: $K^+p \to K^+p\pi^+\pi^-$. Dashed lines: $K^+p \to K^+p2(\pi^+\pi^-)$. Dotted line: $K^+p \to K^+p3(\pi^+\pi^-)$.

ponding data for K^-p reactions in Fig. 5. The data in the available energy range show that $\langle b_W^2 \rangle^{1/2}$ is at most of the order of 0.4 fm and decreases for higher multiplicity reactions. For reaction (a) the bound is almost energy independent between 16 GeV/c and 32 GeV/c, whereas it increases monotonically for reactions (b) and (c), if for the latter we assume that K^+ and K^- interactions behave similarly.

We have also calculated the Webber bounds with the slightly different expression for $\langle b_W^2 \rangle$ used in Ref. 20. The results almost coincided with those given in Table II and are not presented.

2. *Henyey-Pumplin bounds*

In applying the HP method, one should optimize the bound by a judicious choice of the arbitrary functions u_i. As our best choice we adopted the functions u_i determined from (13).[36]

As an example, we show in Fig. 6 the τ distribution for reactions (a) and (b) at 32 GeV/c together with the result of the fit using expression (16). The HP bounds obtained by averaging (15) over all events are collected in Table II.[37] Contrary to expectations,[14] one notices that the HP method does not lead to bounds significantly different from the Webber bounds, although the former are superior in principle. The possibility of strong absorptive effects is therefore not supported by our data.

As a test of the HP (and Webber) method, we determined the HP bounds for events generated by Monte Carlo according to model (2), with β_i values from Table I. Since the real rms impact parameter for this model is equal to the already calculated "minimum bound," this procedure allows us to check the validity of the technique. The results, presented in Table II, column (6) show that the HP method may be somewhat less efficient

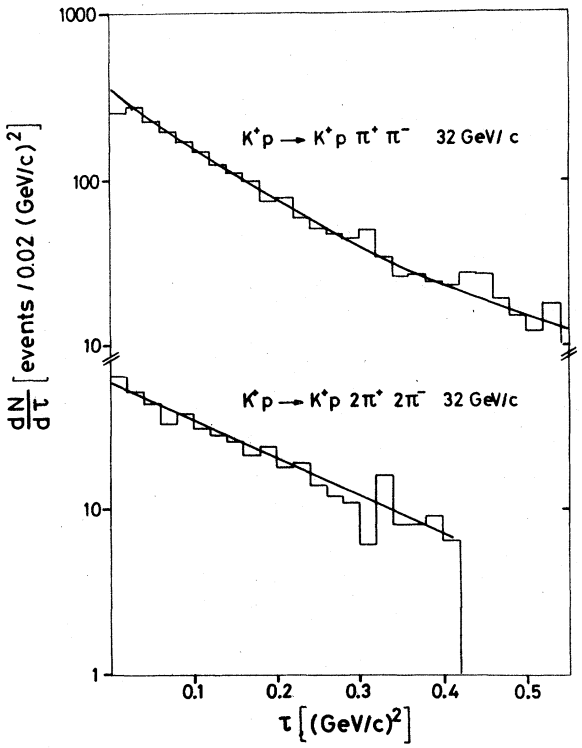

Fig. 6. Distributions of the τ variable for reactions (a) and (b) at 32 GeV/c. The curves represent a polynomial fit to $\ln(d\sigma/d\tau)$. τ is defined by expression (14), see text.

than expected. Moreover, it should be noted that the model HP bounds agree within a few standard deviations with the experimental ones.

The same Monte Carlo events were also used to evaluate the HP bound with a technique applied in Ref. 38. These authors chose the smallest value $\tau_{\min}$, out of the n τ values for each event, to construct the distribution $d\sigma/d\tau_{\min}$ and obtained significantly larger values for the HP bounds than the ones obtained by the Webber technique. Comparison of our results, obtained with this method (Table II, column 7) with the exact rms impact parameter (column 3) proves that the $\tau_{\min}$ procedure is incorrect.

3. *Determination of the "maximum bound"*

Although the Webber and HP techniques are model independent, possibly higher bounds may be obtained by considering phenomenological models which successfully describe the relevant experimental data. For this reason we used the uncorrelated model of Sec. II C to evaluate the overlap function. Since this model takes all rapidity correlations into account, including leading particle effects, and describes the rapidity dependence of transverse-momentum correlations rather well, one expects the resulting bound to be higher than the Webber or HP bound and essentially equal to the "maximum bound."

At fixed rapidities y_i, the overlap function for this model is given by[34]

$$F_n(y_1, \ldots, y_n, t) = \exp\left(\frac{t}{8}\sum_{i=1}^{n} x_i^2/a_i^2(y_i)\right) \qquad (17)$$

and can be evaluated event by event.

The lower bounds obtained by averaging over all events of reactions (a) and (b) are presented in Table II, column 8,[39] and in Fig. 5. For reaction (c) at 32 GeV/c, statistics were insufficient to apply the overlap function technique. Comparison with the previously discussed bounds shows that the new ones are only slightly but systematically higher than the corresponding Webber or HP bounds and moreover agree well with the "minimum bounds."

The same method was used to make a differential study of reaction (a) where the statistics is highest. In Table III we show values of the bounds in the (x_+, x_-) plot, where x_+ (x_-) is the Feynman

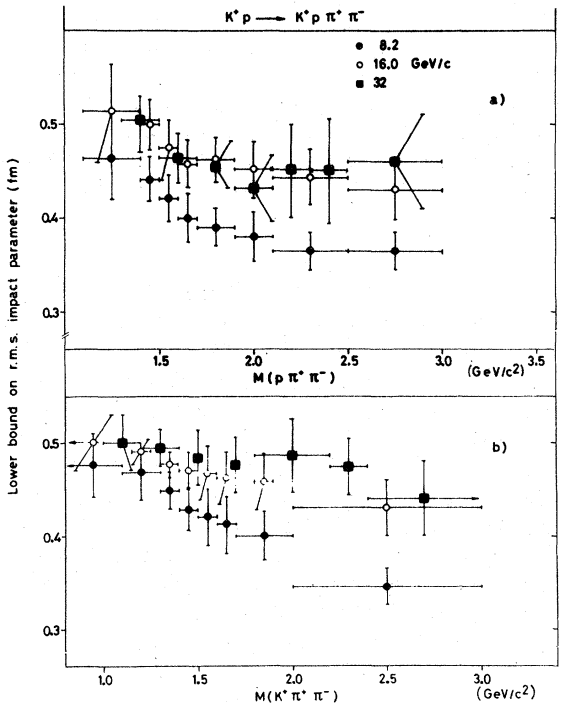

FIG. 7. Dependence of lower bounds of reactions (a) at 8.2, 16, and 32 GeV/c on (a) effective mass of the $(p\pi^+\pi^-)$ system (b) effective mass of $(K^+\pi^+\pi^-)$ system, with selection on $\Delta^{++}(1236)$ and $K^{*\circ}$ (890) as described in text.

TABLE III. Lower bounds in fm obtained with the overlap-function method for intervals in longitudinal momentum x_+ (x_-) of the positive (negative) pion in the reaction $K^+p \to K^+p\,\pi^+\pi^-$ at (a) 8.2, (b) 16, and (c) 32 GeV/c.

(a) 8.2 GeV/c

x_- \ x_+	(−1.0)−(−0.5)	(−0.5)−(0.25)	(−0.25)−0.0	0.0−0.25	0.25−0.5	0.5−0.75	0.75−1.0
(−1.0)−(−0.5)			0.38±0.08	0.35±0.07	0.33±0.15	0.37±0.19	
(−0.5)−(−0.25)		0.36±0.07	0.35±0.03	0.35±0.04	0.29±0.08	0.35±0.08	
(−0.25)− 0.0	0.35±0.08	0.36±0.03	0.40±0.02	0.41±0.02	0.41±0.03	0.43±0.04	0.41±0.10
0.0− 0.25	0.36±0.06	0.37±0.02	0.43±0.02	0.43±0.02	0.41±0.02	0.44±0.03	0.43±0.19
0.25− 0.5	0.34±0.08	0.32±0.03	0.39±0.02	0.42±0.02	0.43±0.02	0.45±0.09	
0.5− 0.75	0.38±0.09	0.36±0.03	0.42±0.02	0.45±0.02	0.43±0.11		
0.75− 1.0		0.41±0.07	0.45±0.05	0.49±0.11			

(b) 16 GeV/c

x_- \ x_+	(−1.0)−(−0.5)	(−0.5)−(0.25)	(−0.25)−0.0	0.0−0.25	0.25−0.5	0.5−0.75	0.75−1.0
(−1.0)−(−0.5)			0.42±0.07	0.40±0.08	0.36±0.13	0.38±0.12	0.45±0.2
(−0.5)−(−0.25)		0.40±0.06	0.40±0.02	0.39±0.14	0.33±0.06	0.36±0.06	0.42±0.09
(−0.25)− 0.0	0.42±0.08	0.41±0.02	0.45±0.01	0.45±0.02	0.45±0.02	0.45±0.02	0.45±0.05
0.0− 0.25	0.41±0.07	0.41±0.02	0.47±0.02	0.48±0.01	0.46±0.01	0.48±0.02	0.48±0.06
0.25− 0.5	0.36±0.11	0.35±0.03	0.42±0.02	0.45±0.01	0.46±0.02	0.47±0.06	
0.5− 0.75	0.40±0.11	0.39±0.03	0.45±0.02	0.48±0.02	0.47±0.06		
0.75− 1.0		0.43±0.05	0.49±0.03	0.51±0.06			

(c) 32 GeV/c

x_- \ x_+	(−1.0)−(−0.5)	(−0.5)−0.0	0.0−0.5	0.5−1.0
(−1.0)−(−0.5)		0.38±0.06	0.37±0.12	0.44±0.17
(−0.5)− 0.0	0.39±0.10	0.39±0.01	0.43±0.03	0.46±0.04
0.0− 0.5	0.39±0.07	0.41±0.02	0.45±0.01	0.48±0.02
0.5− 1.0	0.42±0.12	0.45±0.03	0.48±0.03	

variable for the positive (negative) pion. The bounds are nearly constant over this plot except for the "diffractive" ($K^+\pi^+\pi^-$) region where slightly but systematically higher values are observed. A similar effect, now also for the ($p\pi^+\pi^-$) system, is seen in Fig. 7, where the bounds are plotted as a function of the effective mass of the "diffractive" ($K^+\pi^+\pi^-$) and ($p\pi^+\pi^-$) systems.[40] The effective-mass dependence of the lower bounds is quite weak when compared with the mass dependence of the slope of the invariant momentum-transfer distributions to the corresponding systems, which exhibits the well-known strong slope-mass correlation.[41]

IV. DISCUSSION AND CONCLUSIONS

(a) In the previous sections various methods were used to determine lower bounds on the rms impact parameter of exclusive K^+p reactions at 8.2, 16, and 32 GeV/c. From the results presented it is evident that all methods are essentially equivalent and provide lower bounds which differ only in detail. The reason for this lies in the structure of the reaction matrix element which was shown to be well approximated by a Gaussian in transverse momenta, at least at fixed rapidities. For such transverse momentum dependence, Webber's and Henyey-Pumplin's method lead to lower bounds which almost coincide with the "minimum" and "maximum" bounds defined previously.

(b) The role of leading particles is clarified by a comparison of the results in Table II, columns (3) and (8). Indeed, while the former are obtained from a model without leading particles and dynamical rapidity correlations, the latter follow from a model which incorporates the complete experimental longitudinal structure of the data. The good agreement between both sets of results

explicitly demonstrates the well-known fact that the forward slope of the overlap function is in general only weakly dependent on the longitudinal-momentum structure of the events. This is also reflected in the small difference between the experimental and predicted values of the variable $\lambda = \langle \sum \beta_i x_i^2 \rangle$, shown in Table I. We therefore conclude that the lower bounds are almost solely determined by the transverse-momentum dependence of the reaction matrix element, a result quite contrary to the intuitive notion of peripherality where most importance is attached to the longitudinal structure of the events.

(c) The dependence of the bounds on multiplicity and incident energy follows the behavior of the variable λ, as may be seen from Fig. 5 or Table II. While the values of β_i obviously reflect dynamics, λ itself is, for given β_i, almost completely determined by properties of cylindrical phase space (see Table I) which produce a decrease of the bounds when multiplicity increases. Similar phase-space effects determine the energy behavior. Reaction (a) is remarkable in this respect since β_p decreases between 16 and 32 GeV/c while β_K and β_π stay almost constant. Since $\langle \sum x_i^2 \rangle$ grows with energy, the net result is an approximately constant lower bound, in striking contrast with the increase observed for the other reactions.

(d) A differential study of reaction (a) shows that the lower bound may be slightly higher in diffractive regions than elsewhere. Nevertheless, the effective mass dependence is much weaker than the well-known slope-mass correlation.

(e) The rms impact parameter of inelastic collisions deduced from elastic K^+p scattering data at our energies[3] is approximately equal to 0.76 fm, while the lower bounds obtained in our analysis are at most of the order of 0.45 fm. Although comparison of lower bounds for exclusive channels with the sum over all inelastic processes is perhaps not very meaningful, the results seem to suggest that spin and/or phase structure of the reaction amplitude contribute considerably to the value of the rms impact parameter, as concluded by Michejda many years ago.[5] Any discussion of peripheral or central production mechanisms based on measurements of momentum distributions loses much of its physical interest if this is indeed the case. However, if phases are really as strongly momentum dependent as the experimental lower bounds on the rms impact parameter suggest, it is conceivable that very-high-resolution studies of interference effects between identical particles (the so-called Bose-Einstein correlations) which depend on phases and are related to the angular momentum of final-state particles[29] might eventually lead to some progress in the study of impact-parameter dependence of hadronic exclusive reactions.

ACKNOWLEDGMENTS

We are grateful for the assistance of the staff of the IHEP accelerator and Mirabelle bubble-chamber crew, and we thank our scanning and measuring teams for their contribution to this experiment. We also thank the Birmingham-Brussels-CERN-Orsay-Saclay Collaboration for permitting us to use their K^+p data at 8.2 and 16 GeV/c.

APPENDIX

This section summarizes some analytical results which were used in our comparison of model (4) with experiment. To simplify the notation we write all expressions for particle 1 and the pair (1, 2).

(i) Single-particle transverse-momentum distributions.

$$\frac{1}{\sigma_n}\frac{d\sigma_n}{d^2k_1 dy_1 \cdots dy_n} = \frac{1}{2\pi}\frac{A^2(1,n)}{A^2(2,n)}\frac{1}{a_1^2(y_1)}F \times \exp\left[-\frac{k_1^2}{2}\left(\frac{1}{A^2(2,n)}+\frac{1}{a_1^2(y_1)}\right)\right], \quad \text{(A1)}$$

with

$$A^2(j,n) = \sum_{i=j}^{n} a_i^2(y_i),$$

$$F \equiv F(y_1, \ldots, y_n), \quad \text{(A2)}$$

(ii) Average transverse momentum squared as a function of rapidity.

$$\langle k_1^2(y_1)\rangle = \frac{2a_1^2(y_1)}{F(y_1)}\sum_{j=2}^{n}\int dy_j a_j^2(y_j) \times \int dy_{j+1}\cdots dy_n \frac{F}{A^2(1,n)}, \quad \text{(A3)}$$

with

$$F(y_1) = \int dy_2 \cdots dy_n F(y_1 \cdots y_n). \quad \text{(A4)}$$

(A3) was used to determine $a_i^2(y_i)$ for each particle type by an iterative process. As starting values we used $a_{i0}^2(y_i) = n\langle k_i^2(y_i)\rangle/2(n-1)$.

(iii) Average scalar product $\langle \vec{k}_1 \cdot \vec{k}_2 \rangle$ at fixed (y_1, y_2)

$$\langle \vec{k}_1 \cdot \vec{k}_2 \rangle_{y_1, y_2} =$$

$$= \frac{-2 \int a_1^2(y_1) a_2^2(y_2) F / A^2(1,n) dy_3 \cdots dy_n}{\int F(y_1, y_2 \cdots y_n) dy_2 \cdots dy_n} , \tag{A5}$$

(iv) Distribution of $Z = \vec{k}_1 \cdot \vec{k}_2$ at fixed y_i, $i = 1, \ldots, n$.

$$\frac{1}{\sigma_n} \frac{d\sigma^n}{dZ dy_1 \cdots dy_n}$$

$$= \frac{1}{2} \frac{A^2(1,n)}{A^2(3,n)} \frac{F}{(p+q^2)^{1/2}} \exp\{-\gamma[q \pm (p+q^2)^{1/2}]\} , \tag{A6}$$

where the plus (minus) sign applies to positive (negative) Z.

$$\gamma = Z / a_1^2(y_1) a_2^2(y_2) ,$$

$$p = \frac{a_1^2(y_1) a_2^2(y_2)}{A^2(3,n)} ,$$

$$q = \frac{a_1^2(y_1) a_2^2(y_2) A^2(1,n)}{A^2(3,n)} , \tag{A7}$$

(v) For completeness we also give the expression for the distribution of the azimuthal angle ψ between transverse momenta $\vec{k}_1$ and $\vec{k}_2$[29]:

$$\frac{1}{\sigma_n} \frac{d\sigma_n}{d\psi dy_1 \cdots dy_n} = \frac{1}{\pi} \frac{A^2(1,n) A^2(3,n) F}{C_1 C_2} G(x) , \tag{A8}$$

with

$$G(x) = \frac{1}{1-x^2} \left(\frac{x}{(1-x^2)^{1/2}} (\arcsin x - \pi/2) + 1 \right) , \tag{A9}$$

and

$$x = \beta \cos\psi / (C_1 C_2)^{1/2} ,$$

$$\beta = 1/2A^2(3,n) , \tag{A10}$$

$$C_i = 1/2a_i^2(y_i) + 1/A^2(3,n) , \quad i = 1, 2 .$$

The azimuthal asymmetry parameter is equal to

$$B(y_1, \ldots, y_n) = \frac{\int_{\pi/2}^{\pi} (d\sigma/d\psi) d\psi - \int_0^{\pi/2} (d\sigma/d\psi) d\psi}{\int_0^{\pi} (d\sigma/d\psi) d\psi}$$

$$= \frac{\beta}{(C_1 C_2)^{1/2}} . \tag{A11}$$

(vi) Overlap function. The slope of the overlap function for a selected class of events is easily obtained from (17) once the functions $a^2(y)$ are found. However, the values resulting from the iteration of (A3) do not reflect the k dependence of the *matrix element* at the edge of the rapidity interval since the $\langle k^2(y) \rangle$ are strongly reduced by phase space in these regions. Straightforward use of such $a^2(y)$ would result in dramatically overestimated and completely unreliable lower bounds, as may also happen in the case of the Webber or HP bound. The following procedure was therefore adopted. Iterated $a^2(y)$ were used only in a central rapidity interval where the phase-space influence was weak. This was verified by Monte Carlo calculation. For the other y regions, we have chosen constant $a^2(y)$, different for each particle and incident momentum, which reproduced sufficiently well the rapidity dependence of $\langle k_i^2 \rangle$ in those y intervals. The overlap function was then evaluated with the modified $a^2(y)$.

The errors quoted in Table II, column 8 take into account errors on $\langle k^2(y) \rangle$ in each interval as well as the statistical error on the average overlap function slope. Study of fluctuations in the results when subsets of data were analyzed independently or when different y intervals were chosen showed that the systematical errors resulting, e.g., from the iteration procedure are comparable or sometimes slightly larger than the statistical errors quoted in the tables.

*Also at Universitaire Instelling Antwerpen, B2610 Wilrijk, Belgium.

[1]U. Amaldi, in *Laws of Hadronic Matter*, Proceedings of the International School of Subnuclear Physics, "Ettore Majorana," Erice, 1973, edited by A. Zichichi (Academic, New York 1975), p. 673.

[2]E. H. de Groot and H. I. Miettienen, in *The Pomeron*, proceedings of the VIII Rencontre de Moriond, Méribelles-Allues, 1973, edited by J. Trân Thanh Vân (CNRS, Paris, 1973).

[3]D. S. Ayres *et al.*, Phys. Rev. D 14, 3092 (1976).

[4]G. Warren *et al.*, Nucl. Phys. B97, 381 (1975).

R. Henzi *et al.*, Nucl. Phys. B16, 1 (1970). V. Barger, K. Geer, and F. Halzen, Nucl. Phys. B44, 475 (1972).

[5]L. Michejda, Nucl. Phys. B4, 113 (1968); Fortschr. Phys. 16, 707 (1968).

[6]L. Van Hove, Nuovo Cimento 28, 798 (1963); Rev. Mod. Phys. 36, 655 (1964).

[7]Z. Koba and M. Namiki, Nucl. Phys. B8, 413 (1968).

[8]Z. Ajduk and R. Stroynowski, Phys. Lett. 30B, 179 (1969).

[9]Z. Ajduk, Nuovo Cimento 16A, 111 (1973).

[10]R. Hwa, Phys. Rev. D 8, 1331 (1973).

[11]A. Bialas and N. Sakai, Phys. Lett. 55B, 81 (1975).

[12]P. Grassberger and J. Kubar-Andre, Nucl. Phys. B116, 285 (1976).

[13]B. Webber, Phys. Lett. 49B, 474 (1974).
[14]F. S. Henyey and J. Pumplin, Nucl. Phys. B 117, 235 (1976).
[15]A. Krzywicki, Nucl. Phys. B86, 296 (1975).
[16]D. Weingarten, Phys. Rev. D 11, 1924 (1975).
[17]P. Grassberger and H. Miettinen, Nucl. Phys. B89, 101 (1975).
[18]The average taken over all reaction channels determines a lower bound on the elastic scattering slope as a consequence of unitarity.
[19]B. R. Webber *et al.*, Nucl. Phys. B97, 317 (1975).
[20]P. Bosetti *et al.*, Nucl. Phys. B97, 29 (1975).
[21]G. Warren *et al.*, Nucl. Phys. B97, 381 (1975).
[22]E. Simopoulou *et al.*, Nucl Phys. B103, 39 (1976).
[23]H. Braun *et al.*, Phys. Rev. D 15, 1293 (1977).
[24]T. Hofmokl *et al.*, Nucl. Phys. B129, 19 (1977).
[25]F. Grard *et al.*, Nucl. Phys. B102, 221 (1976); A. Stergiou *et al.*, *ibid.* B102, 1 (1976).
[26]To show this explicitly, we recalculated λ for a model with matrix element $|M^1|^2 = |M|^2 (E^p - p_L^p)(E^K + p_L^K)^{1/2}$ and $\beta_i = 4$ (GeV/c)$^{-2}$ which simulates strong leading-particle effects. E^p, p_L^p (E^K, p_L^K) are c.m.s. energy and longitudinal momentum of the proton (kaon). We obtained $\lambda' = 5.332 \pm 0.008$ (GeV/c)$^{-2}$ for reaction (a) at 32 GeV/c to be compared to $\lambda = 5.136 \pm 0.004$ (GeV/c)$^{-2}$ when leading-particle effects were omitted. The difference $|\lambda' - \lambda|$ is even smaller for higher-multiplicity reactions.
[27]C. Michael, Phys. Lett. 57B, 379 (1975).
[28]A detailed analysis of so-called "azimuthal correlations" in reaction (b) at 16 GeV/c has already been published; see Ref. (29) where further references to the literature on this subject may be found.
[29]E. De Wolf *et al.*, Nucl. Phys. B132, 383 (1978).
[30]A. Bialas *et al.*, Nucl. Phys. B86, 365 (1975).
[31]However, very short-range transverse-momentum correlations between like-pion pairs where shown to exist in reaction (b) at 16 GeV/c (Ref. 19). These are not likely to influence appreciably the results to be discussed in following sections.
[32](a) M. Le Bellac, Academic Training Programme Lecture Notes, CERN 76-14, 1976 (unpublished); (b) D. Weingarten et al., Phys. Rev. Lett. 37, 1717 (1976).
[33]For simplicity we neglect spins of the incident particles.
[34]C. S. Lam and R. T. Sharp, Phys. Rev. D 8, 278 (1973).
[35]Strictly speaking, the bounds presented in Table II, column 3 are not the smallest possible ones since we calculated the overlap function slope with constant β_i values. However, the rather good agreement between model (2) and the experimental $\langle k_i^2(y_i)\rangle$ values shows that this approximation should not significantly affect the values of the "minimum bounds."
[36]We also calculated the HP bounds for the choices $u_i = x_i$ and for $u_i = x_i/\langle k_i^2(x_i)\rangle$, where $\langle k_i^2(x_i)\rangle$ is the experimental average k_i^2 in a small interval around x_i. The resulting bounds were not significantly different from the ones described in the text.
[37]Compatible results were found by numerical integration of (15). Errors on Webber and HP bounds were estimated using a Monte Carlo technique in which the experimental averages (Webber) or fitted parameters (HP) were distributed according to a Gaussian with average and dispersion equal to the experimental value or fitted parameter and error, respectively.
[38]Aachen-Berlin-Bonn-CERN-Cracow-Heidelberg-Warsaw Collaboration, paper 466 submitted to the International Conference on High Energy Physics, Budapest, 1977 (unpublished).
[39]See the Appendix for a discussion of some important technical details.
[40]The "diffractive" events were selected by the following cuts: $(p\pi^+\pi^-)$ system: $1.16 < M(p\pi^+) < 1.32$ GeV/c^2 and $M(K^+\pi^-) < 0.84$ GeV/c^2 or $M(K^+\pi^-) > 0.94$ GeV/c^2, $(K^+\pi^+\pi^-)$ system: $0.84 < M(K^+\pi^-) < 0.94$ GeV/c^2 and $M(p\pi^+) > 1.32$ GeV/c^2.
[41]J. N. Carney *et al.*, Nucl. Phys. B110, 248 (1976).